

DETECTORS AND BEAM MONITORS BASED ON WIDE BANDGAP SEMICONDUCTORS AT CRYOGENIC TEMPERATURES*

S. V. Kuzikov[†], Thomas Jefferson National Accelerator Facility, Newport News, VA, USA
 G. Burrows, University of Kentucky, Lexington, KY, USA

Abstract

Wide-bandgap semiconductors, such as single-crystal diamond and sapphire, can be used to measure the flux of passing particles through a particle-induced conductivity effect. We recently demonstrated a diamond-based, electrodeless electron beam halo monitor. This monitor utilized a thin diamond blade placed within an open, high-quality microwave resonator. The blade partially intercepted the beam and changes in the RF properties of the resonator were used to infer beam parameters. To enhance the sensitivity of our semiconductor sensors, we propose two new techniques: (1) biasing the semiconductor sensor to support avalanche multiplication of free carriers, and (2) operating at cryogenic temperatures to reduce intrinsic semiconductor losses and increase the mobility of induced carriers. These techniques are applicable not only to particle beam diagnostics but also to the detection of various types of ionizing radiation.

INTRODUCTION

Wide-bandgap semiconductors, such as diamond and sapphire, can transit from dielectric to "metallic" states through photo- or beam-induced conductivity. When high-energy photons or beam particles strike the semiconductor, they generate secondary charge carriers (electrons and holes) in the conduction band, increasing the overall conductivity of the crystal. This phenomenon allows the measurement of primary photon or particle beam fluxes by detecting changes in the semiconductor's conductivity.

The proposed method involves placing a semiconductor sample inside an open, high-quality, critically coupled RF resonator, which is highly sensitive to changes in inserted losses (Fig. 1). Variations in the resonator's reflection coefficient—quantified by the S_{11} parameter—can be precisely measured.

The described principle was successfully implemented by Euclid Techlabs under a DoE SBIR grant [1–4]. Experiments conducted at Argonne Wakefield Accelerator (AWA) using a diamond beam halo monitor demonstrated greater sensitivity than traditional YAG screens and enabled two-dimensional mapping of the beam density distribution. By employing a novel nonlinear response processing method and multi-pixel beam image reconstruction, high space resolution was also achieved [4].

Additionally, an avalanche effect—previously observed in classical diamond sensors [4]—was discovered in this RF-based technology, significantly enhancing sensitivity. In this process, free carriers induced in diamond drift under

a DC bias electric field and, through collisions, generate new secondary carriers. This chain reaction (or avalanche) results in a much higher concentration of carriers compared to the unbiased case, increasing detector sensitivity by up to two orders of magnitude.

A key advantage of this technique lies in the high-quality factor (Q-factor) of the RF resonator containing the semiconductor. For the best single-crystal diamond samples at room temperature, the loss tangent (10^{-3} to 10^{-4}) limits the Q-factor of the RF cavity. To overcome this limitation, we propose using an RF resonator incorporating a diamond or sapphire element cooled to cryogenic temperatures, which can increase detection sensitivity by several orders of magnitude.

RF MEASUREMENT TECHNIQUE

When exposed to beam particles or high-energy photons, the dielectric permittivity of wide bandgap semiconductors increases significantly in the imaginary component, indicating heightened conductivity due to the generation of secondary charge carriers:

$$\epsilon = \epsilon' + i\epsilon' \tan\delta + i\frac{4\pi\sigma}{\omega}, \quad (1)$$

where ϵ' is real part of permittivity, $\tan\delta$ is loss tangent, ω is RF frequency, and σ is crystal conductivity induced by primary particles. The dielectric response of a semiconductor can be described by this complex permittivity consisting of three components. The first term corresponds to the real part of the dielectric constant, which is approximately 5.7 for diamond and 9.4 for sapphire. The second term represents the imaginary part, or the material's natural loss tangent, which varies with both frequency and temperature. The third term accounts for beam- or photon-induced conductivity and is proportional to the density of free secondary charge carriers (electrons and holes), denoted as N_e :

$$\sigma = eN_e(\mu_e + \mu_h). \quad (2)$$

Here, μ_e and μ_h represent the mobilities of electrons and holes in the conduction band, respectively. The induced free carrier density, N_e , is proportional to the density of the incident primary particles but also depends on their energy and depth of penetration into the material.

At cryogenic temperatures, both diamond and sapphire exhibit exceptional performance characteristics. Diamond possesses extraordinarily high mobilities for free carriers. At 10 K, the electron mobility in diamond reaches approximately $1 \times 10^6 \text{ cm}^2 \text{V}^{-1} \cdot \text{s}^{-1}$ —three orders of magnitude higher than at room temperature (300 K) [5]. This enhanced mobility enables much higher induced conductivity at temperatures 70 K and below, and thus, significantly improved sensitivity to primary particle exposure (Fig. 2). In

*This material was supported by the U.S. Department of Energy, Office of Science, Office of Nuclear Physics (contract DE-AC05-06OR23177).
 † kuzikov@jlab.org

this simulation we considered a 10 GHz closed TE₁₀₁ resonator at 10 GHz with copper walls and diamond size of 5×5×0.5 mm³. We accounted for loss tangent and copper conductivity dependence on temperature.

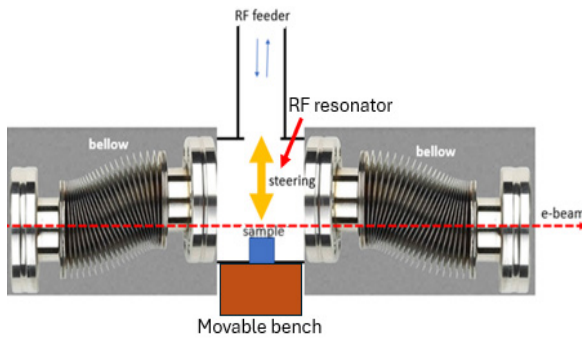


Figure 1: Halo monitor based on steering resonator on movable bench.

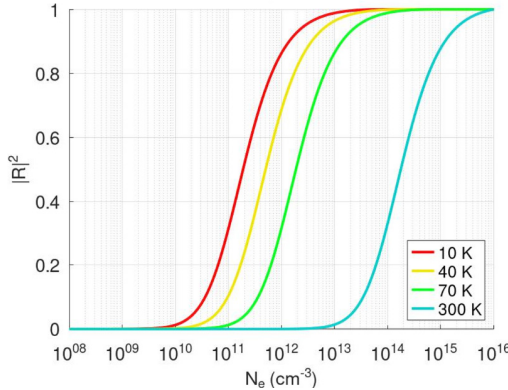


Figure 2: Reflectivity of a 10 GHz resonator with diamond sensor.

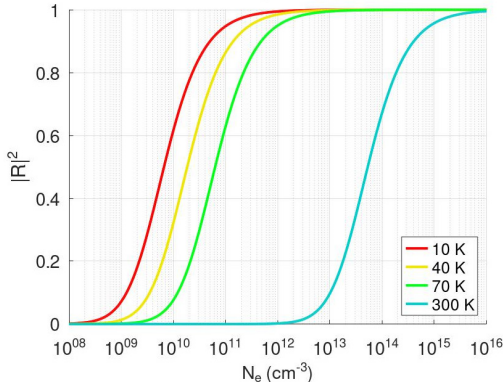


Figure 3: Reflectivity of a 10 GHz resonator with sapphire sensor.

Sapphire also shows outstanding behavior at low temperatures. While its loss tangent in the X-band is around 10⁻⁵ at room temperature, it decreases dramatically to as low as 10⁻¹⁰ at 10 K [6-8]. This ultra-low loss enables Q-factors comparable to those of superconducting cavities, forming the basis of achieving unprecedented detection sensitivity that is shown in Fig. 3 for the same TE₁₀₁ resonator.

In fact, the minimum measurable induced conductivity is defined by the condition in which the beam-induced

imaginary component of the permittivity becomes comparable to the material's natural imaginary permittivity—i.e., the level determined by the intrinsic loss tangent.

$$\sigma_{min} \leq \frac{10^{-10}}{4\pi} \tan\delta \cdot \omega \epsilon'. \quad (3)$$

At 1 GHz and 10 K, a sapphire-based RF resonator can detect conductivity levels as low as 10⁻¹¹ S/m. In contrast, conventional techniques rely on measuring the current flowing through a semiconductor [9-10]. These techniques are typically limited to detecting conductivities. This limitation is set by the minimum measurable current, I_{min} , in the detection system:

$$\sigma_{min} = \frac{I_{min}}{Ud}, \quad (4)$$

where U is applied voltage and d is thickness of the sample. For $I_{min}=1$ nA, $U=1$ kV, and $d=0.5$ mm, we obtain $\sigma_{min}=10^{-9}$ S/m.

CST SIMULATIONS

Beam Halo Monitor

We performed simulations to estimate the carrier density, N_e in a diamond blade exposed to the CEBAF beam, using beam parameters taken from [11]. The density N_e is given by:

$$N_e = \frac{q}{e} \frac{E_0(1-e^{-\frac{a}{d_p}})}{\pi ar_b^2 W_{e-h}(1-e^{-\frac{1}{\tau f_{rep}}})}, \quad (5)$$

where q is bunch charge (0.3 pC), e is charge of electron, a is blade size (5 mm), r_b is beam radius (0.5 mm), E_0 is energy of beam particles, d_p is penetration depth, τ is relaxation time of carriers (500 ns), f_{rep} is repetition rate of bunches (400 MHz), and W_{e-h} is energy to create electron-hole pair (13 eV).

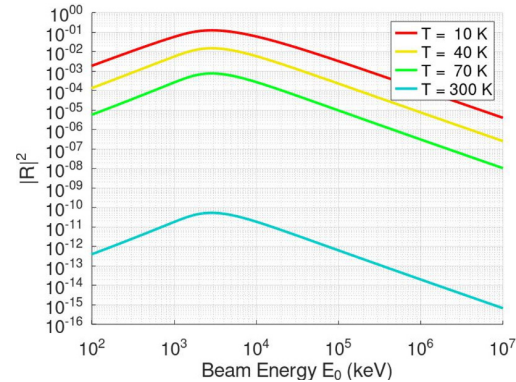


Figure 4: Reflectivity of TE₁₀₁ resonator with sapphire blade vs beam energy at four different temperatures.

For the case in which carrier density in the beam core is 10⁶ times the particle density in the beam halo, the carrier density induced by halo in diamond can reach approximately 10¹⁰ cm⁻³. The maximum energy deposition in the diamond corresponds to a beam energy of about 10 MeV, since the penetration depth d_p increases with beam energy following the relation $d_p \sim E_0^n$, $n = 1.67$. At this energy, the

penetration depth matches the longitudinal size of the blade, resulting in maximum creation of free carriers [12].

In case of sapphire blade instead of diamond, the corresponding reflection from the resonator is shown in Fig. 4. The reachable reflectivity at 70 K is high enough for RF measurements in a broad range of beam energies.

We have developed a preliminary design for an RF resonator incorporating a diamond blade operating at 70 K (Fig. 5). The designed resonator operates in the TM_{211} mode. The predicted reflection signal, shown in Fig. 6, falls well within the measurable range.

We also propose using a movable bench, a motorized piezoelectric XYZ stage, that operates in air, while keeping the scanning resonator enclosed in vacuum with nanometer-scale precision (Fig. 1).

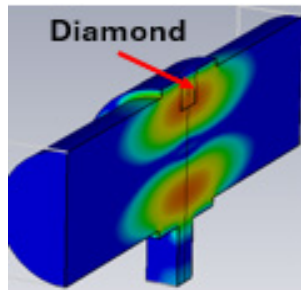


Figure 5: E-field in TM_{211} resonator with diamond blade sensor at 70 K.

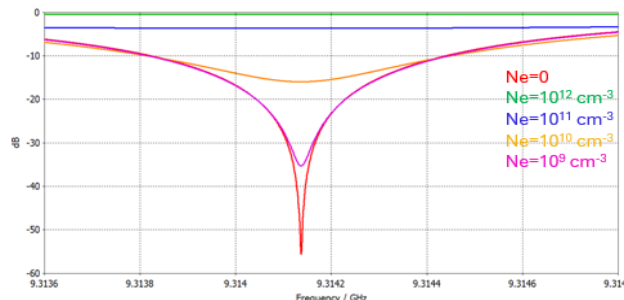


Figure 6: S_{11} parameter vs frequency for several densities of carriers.

X-ray Detector

Another device to be developed as part of this project is a compact X-ray detector, which can be integrated with the microcooler [13]. This rapid device can reach 70 K within several minutes. The RF design of the X-ray detector differs significantly from that of the beam halo monitor. Instead of a thin blade, a bulk semiconductor is preferred to increase the probability of free carrier generation as X-ray photons pass through the material.

Figure 7 presents our preliminary design based on a sapphire cylindrical insert operating in the TM_{011} mode. Critical coupling was achieved by adjusting the distance between the coaxial rod and the sapphire cylinder. Notably, at 70 K, the reflection signal is measurable for carrier densities as low as 10^7 cm^{-3} (Fig. 8). Additionally, a bias voltage can be applied between the coaxial rod and the resonator walls to induce an avalanche regime, further enhancing sensitivity.

CONCLUSION

We propose a novel detection technique based on highly sensitive RF technology. Maximum sensitivity is achieved by using a cryogenic host resonator containing diamond or sapphire samples. When particles or X-rays induce conductivity in these semiconductors, the resulting changes in the sample's electrical properties are detected through variations in the S-parameters of the host resonator. Operating at cryogenic temperatures enables exceptionally high carrier mobilities and Q-factors of the host resonators, which together provide the ultra-high sensitivity that defines the strength of this method.

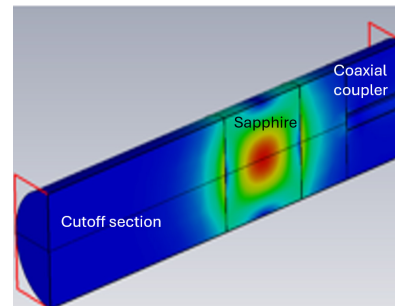


Figure 7: Field distribution of the operating mode at resonance frequency.

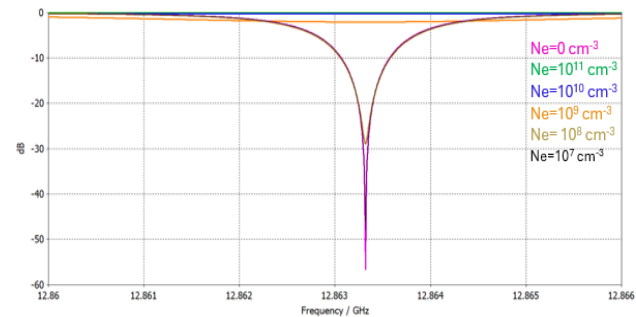


Figure 8: S_{11} parameter vs frequency for several densities of carriers.

REFERENCES

- [1] S.Antipov, *et al.*, "Detection of X-Rays and Charged Particles Via Detuning of the Microwave Resonator", in *Proc. PAC'18*, Vancouver, BC, Canada, Apr.-May 2018, pp. 1958-1960.
doi:[10.18429/JACoW-IPAC2018-WEPAF058](https://doi.org/10.18429/JACoW-IPAC2018-WEPAF058)
- [2] S.V. Kuzikov, *et al.*, "Diamond Beam Halo Monitor", in *Proc. IBIC'20*, Sep. 2020, Santos, Brazil, pp. 197-201.
doi:[10.18429/JACoW-IBIC2020-WEPP38](https://doi.org/10.18429/JACoW-IBIC2020-WEPP38)
- [3] S.V. Kuzikov *et al.*, "Electrodeless Diamond Beam Halo Monitor", in *Proc. IPAC'21*, Campinas, SP, Brazil, May 2021, pp. 2990-2993.
doi:[10.18429/JACoW-IPAC2021-WEPAB164](https://doi.org/10.18429/JACoW-IPAC2021-WEPAB164)
- [4] S.V. Kuzikov *et al.*, "An Electrodeless Diamond Beam Monitor", in *Proc. NAPAC'22*, Albuquerque, NM, USA, Aug. 2022, pp. 904-906.
doi:[10.18429/JACoW-NAPAC2022-THZE3](https://doi.org/10.18429/JACoW-NAPAC2022-THZE3)
- [5] A. Portier *et al.*, "Carrier Mobility up to $106 \text{ cm}^2 \text{ V}^{-1} \text{ s}^{-1}$ Measured in Single-Crystal Diamond by the Time-of-Flight Electron-Beam-Induced-Current Technique", *Phys. Rev.*

- Appl.*, vol 20, p. 024037, 2023.
[doi:10.1103/PhysRevApplied.20.024037](https://doi.org/10.1103/PhysRevApplied.20.024037)
- [6] N. Pogue *et al.*, “Measurement of the dielectric properties of high-purity sapphire at 1.865 GHz from 2-10 Kelvin”, *AIP Conference Proceedings*, Spokane, WA, USA, Jun. 2011, pp. 945-952.
[doi: 10.1063/1.4707011](https://doi.org/10.1063/1.4707011)
- [7] S. N. Buckley *et al.*, “Cryogenic dielectric properties of sapphire at 2.45 GHz”, *J. Phys. D: Appl. Phys.* vol. 27, p. 2203, 1994.
[doi:10.1088/0022-3727/27/10/033](https://doi.org/10.1088/0022-3727/27/10/033)
- [8] F. Wang *et al.*, “Electronic Charge Transport in Sapphire Studied by Optical-Pump/THz-Probe Spectroscopy”, *SPIE Proceedings*, vol. 5352, San Jose, CA, USA, Jan. 2004.
[doi:10.1117/12.532505](https://doi.org/10.1117/12.532505)
- [9] F. Bachmair, “CVD Diamond Sensors in Detectors for High Energy Physics”, Ph.D. Thesis, ETH, Zürich, Switzerland.
[doi:10.3929/ethz-a-010748643](https://doi.org/10.3929/ethz-a-010748643).
- [10] S. Liu *et al.*, “In Vacuum Diamond Sensor Scanner for Beam Halo Measurements in the Beamline at the KEK Accelerator Test Facility”, *Nucl. Instrum. Methods Phys. Res. A*, vol. 832, pp. 231–242, 2016.
[doi:10.1016/j.nima.2016.06.122](https://doi.org/10.1016/j.nima.2016.06.122)
- [11] P. A. Adderley *et al.*, “The Continuous Electron Beam Accelerator Facility at 12 GeV”, *Phys. Rev. Accel. Beams*, vol. 27, p. 084802, 2024.
[doi:10.1103/PhysRevAccelBeams.27.084802](https://doi.org/10.1103/PhysRevAccelBeams.27.084802)
- [12] K. Kanaya and S. Okayama. “Penetration and energy-loss theory of electrons in solid targets”, *J. Phys. D: Appl. Phys.*, vol. 5, p. 43, 1972.
[doi:10.1088/0022-3727/5/1/308](https://doi.org/10.1088/0022-3727/5/1/308)
- [13] J. R. Olson, “Microcryocooler for tactical and space applications”, *AIP Conference Proceedings* vol. 1573, Anchorage, AK, USA, Jun. 2013, pp. 357-364, 2014.
[doi:10.1063/1.4860723](https://doi.org/10.1063/1.4860723)